

# Comparison of Permeability on the Actual and Ideal Cancellous Bone Microstructure

Mohammed Rafiq Abdul Kadir<sup>1</sup> and Ardiyansyah Syahrom<sup>2c</sup>

<sup>1</sup>*Biomechanics & Tissue Engineering Group, Faculty of Biomedical Engineering and Health Science, Universiti Teknologi Malaysia*

<sup>2</sup>*Faculty of Mechanical Engineering, Universiti Teknologi Malaysia*

Received: 25/07/2009 – Revised 07/09/2009 – Accepted 11/09/2009

## Abstract

The synthesis of cancellous bone has a variety of factors to influence the design of trabecular bone including structure, material properties, geometry and permeability. To investigate such relationships, we used a constant flow rate permeameter to determine the intrinsic permeability of trabecular bone. The paper describes an analyses of actual and ideal model of microarchitecture and compares the corresponding permeability to find the similarity of cancellous bone structure that represents actual cancellous bone. In the present simulation, a computational fluid dynamics method was used to analyse fluid flow, the morphology of cancellous bone, the trabecular thickness (Tb.Th), trabecular separation (Tb.Sp), bone volume fraction (BV.TV) and bone surface density (BS/BV). Three different models were analysed; actual model of cancellous bone, prismatic and quadratic crystal shape. The model geometry is 4.5 mm (diameter) and 4 mm (height). Fluid media in the simulation is blood, with a pressure of (15 kPa) and mass flow rate (100 ml/hr). The comparison of three model microstructure is also presented. The results show that prismatic model have similar permeability with actual model of cancellous bone. Quadratic crystal shape was the most grates permeability of cancellous bone.

*Keywords: Cancellous bone; Permeability; Porous media; Mechanobiology transport; Trabecular.*

## 1. Introduction

Osteoporosis is a skeletal disease characterized by low bone mass and microarchitectural deterioration of bone tissue, and is associated with an increase in bone fragility and low-energy fractures [1, 2]. There is a high correlation with low bone mass and increased fracture risk. To repair cancellous bone disease, the orthopedic surgeons have traditional method that includes autograft and allograft. The traditional method has limitations such as donor site morbidity, infection, pain, hematoma, genetic differences, limited donor bone supply, anatomical and structure problems, loss of bone inductive factors and elevated levels of resorption during healing. To reduce some limitation, the surgeons used implantation or artificial cancellous bone with mimicked microarchitecture of trabecular bone.

<sup>c</sup> Corresponding Author: Ardiyansyah Syahrom

Email: [ardiyansyah@utm.my](mailto:ardiyansyah@utm.my) Telephone: +607 5535961

Fax: +607 5566159

© 2009-2012 All rights reserved. ISSR Journals

The synthesis of cancellous bone has a variety of factors to influence of the design including structure, material properties [3], geometry and transport phenomena of trabecular bone. This paper focuses on transport phenomena such as properties of cancellous bone. Marrow movement in cancellous bone will cause shear stress at the trabecular surface. As the cancellous bone deforms according to applied mechanical loads, there should be pressure differences within the cancellous bone. The magnitude of this pressure difference across the cancellous bone will depend on a variety of factors, including bone strain [4, 5], marrow rheology, and bone matrix permeability [6, 7].

The concerned transport phenomena is a pumping mechanism to maintain the hydration and nutrient supply [8] or the movement of bone marrow to the bone. The dominant flow going to pore structure of the cancellous bone can become an alteration of mass transfer properties which is one of the numerous key points of the mechano-biological control loop of the evolution of the pathology [8] or quality of the bone. Cancellous bone and the restorative remodelling response observed in response to disuse cause a thinning of existing trabeculae and a loss of trabecular bone volume with eventual loss of connectivity between trabeculae [4]. The trabecular bone is a self-repairing structure material with biological-nutrients, which adapts its material properties, and shape in response to altered mechanical loading. Bone mass and architecture are regulated by physical activity, and significant changes in bone mass have been observed when physical activity has been reduced or increased [4].

The hydraulic permeability of cancellous bone is function of porosity and viscosity [6, 7, 9-11]. However, very little is known about the permeability of vertebral cancellous bone, especially the interdependence of permeability and porosity. Some researches have investigated the correlation of permeability of cancellous bone based on different locations at anatomic calcaneal [7, 8, 10]. The porosity of cancellous bone is dependent on the structure, anatomic site and direction of cut of the bone. Structure of cancellous bone consists of a continuous three-dimensional network of inter connected rod and plates and a pore space [10, 12, 13]. The porosity also affects the material properties and strength of the structure.

From the previous studies of marrow free specimens vary over six orders of magnitude, it was found that the permeability of cancellous bone is in a range  $3.71 \times 10^{-14}$  to  $1 \times 10^{-8}$  m<sup>2</sup> for human calcaneus [11].

The aim of the present study is therefore to analyse permeability of actual and ideal model of microarchitecture. Our specific objective is to compare permeability of ideal and actual of trabecular bone in order to find the similarity of cancellous bone structure to represent actual cancellous bone.

## **2. Materials and Methods**

Three dimensional model of a cancellous bone was constructed from micro computed tomography ( $\mu$ CT) image data set. The dataset comprised 190 layers of 2D images of trabecular structure in cylindrical form with a diameter of 15mm and a height of 190mm (Fig. 1). The small section was taken out from the cancellous bone sample for analysis with size diameter 4.5mm, height 5mm as in figure 1.

Twenty sub-regions representing one unit cell each were taken out from the cancellous bone sample for parametric analysis. Six indices were chosen to describe the morphology of all the unit cells – the trabecular thickness (Tb.Th), trabecular separation (Tb.Sp), bone volume fraction (BV.TV) [5, 14], Bone surface density (BS/BV), Like-plate trabecular (P) and like-rod trabecular (R) [15-18] as shown in figure 2, and also the porosity of the trabecular part of morphological.

Porosity is a measure of the void spaces in a material, and is measured as a fraction, between 0–1, or as a percentage between 0–100%. Based on the definition, the porosity  $\varepsilon$  of trabecular bone is simply determined by

$$\varepsilon = \frac{V_0 - V}{V_0} \quad (1)$$

where  $V_0$  is the total volume of a single cell and  $V$  is the volume that struts occupy.

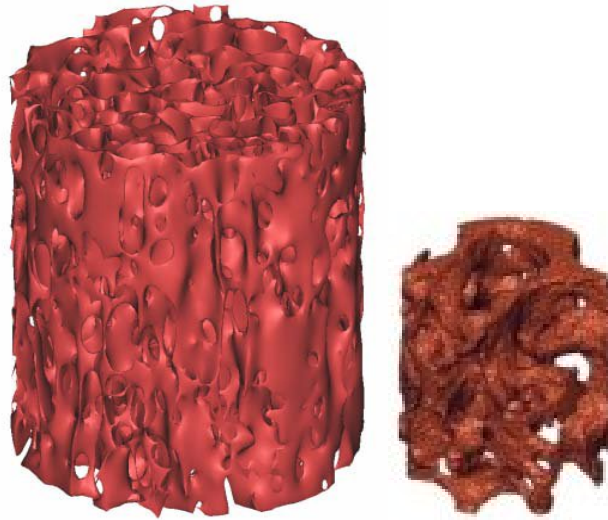


Figure 1. Three dimensional model of a trabecular bone reconstructed from  $\mu$ CT and a section from the model used in the analysis.

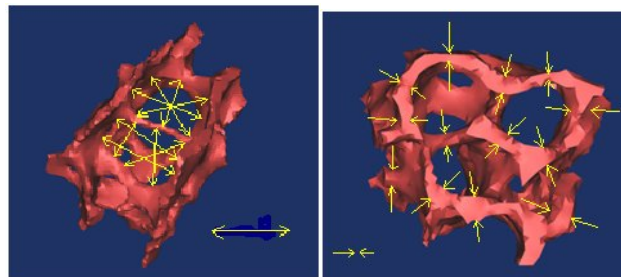


Figure 2. One unit cell of cancellous bone showing the measurement for the morphological indices.

From the morphological indices, two idealised models of trabecular microarchitecture were constructed – the prismatic and the quadratic crystal shape, as in figure 3. All the models were then turned into simulation model. Table 1 shows the actual and idealised models in three different views. This would give a rough idea of how closely the idealized models resembled the actual bone.

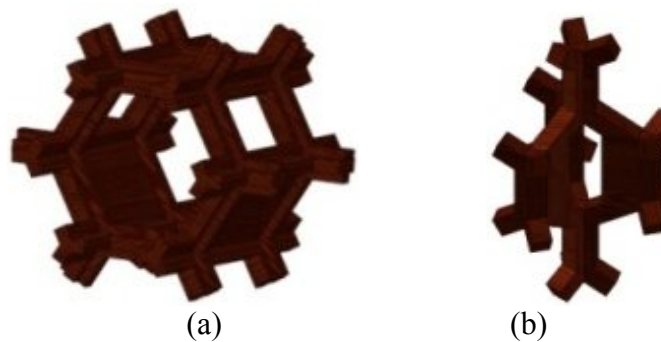
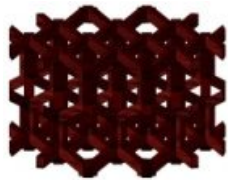
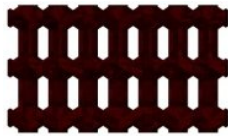
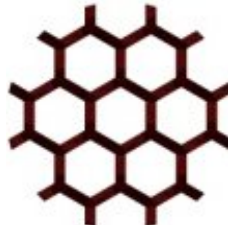
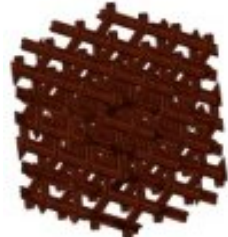


Figure 3. Unit cell of idealized cancellous bone; (a). Prismatic model and (b). Quadratic crystal shape (QCS)

TABLE 1 ACTUAL CANCELLOUS BONE AND THE IDEALIZED MODELS.

Model	Isometric view	Side view	Top view
actual			
Quadratic crystal shape			
Prismatic			

The model simulation was developed using 3D CAD drawing as shown in figure 4. The model has been commonly used in determine permeability of cancellous bone [10]. Cancellous bone model was put at centre of the two cylinder model simulation. Blood were used as fluid media for simulation. The operating pressure is 15 kPa, dynamic viscosity is 0.005 pa.s, temperature of fluid is 37°C [6, 10] and volumetric flow rate is 100 ml/hr [6]. Porous media is dependent on the porosity of material and permeability type is unidirectional. the simulation was performed using static pressure and constants flow rate [11]. A CFD software was used to simulate model of cancellous bone, the model to simulate typical in vitro experiment testing condition (figure 4). For each model, the pressure and velocity value were plotted.

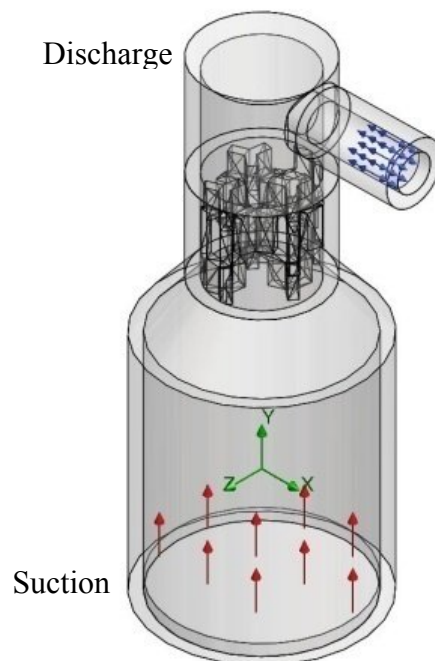


Figure 4. Boundary condition of simulation.

Permeability was calculated using Darcy's law from the equations detailed in [6, 7, 9-11, 19-22]:

$$v_D = \frac{Q}{A_s} = \left( \frac{kA}{\mu} \right) \frac{(P_u - P_d)}{L_s} \quad (2)$$

where  $Q$  is the volumetric flow rate ( $m^3/s$ ),  $A_s$  is the cross-sectional area of the specimen ( $m^2$ ),  $P_u$  is the upstream pressure (Pa),  $P_d$  is the downstream pressure (Pa),  $L_s$  is the specimen length (m),  $\mu$  is the fluid viscosity (0.001 Pa.s for water), and  $k$  is the intrinsic permeability of the specimen ( $m^2$ ).

### 3. Results

Figure 5 shows thickness distribution of cancellous bone, the mean value of trabecular thickness was found to be 0.366mm, ranged from a minimum of 0.084mm to a maximum of 1.89mm. Figure 6 shows cancellous bone separation with ranged from 0.148 to 5.085mm and the mean value is 1.67mm. Average bone volume fraction was 0.322 and bone surface density was  $8.39mm^{-1}$ . Like-plate trabecular was 2.7 and like-rod trabecular was 5.8.

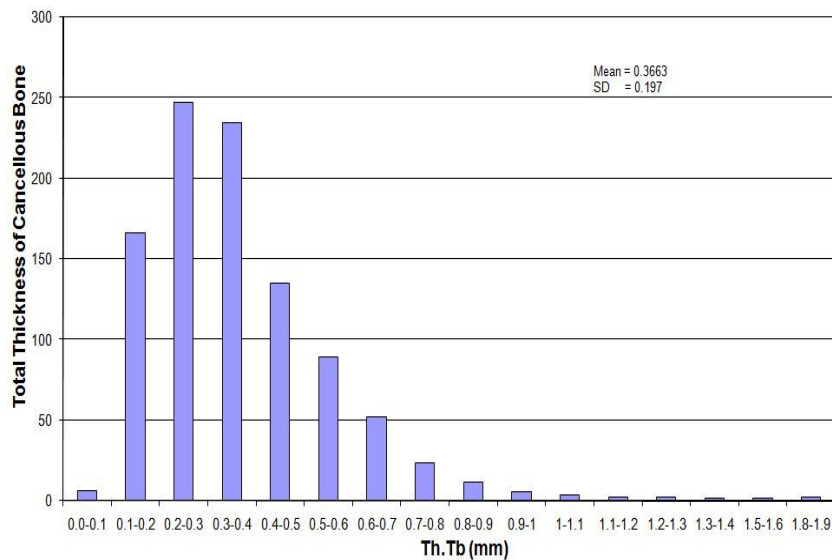


Figure 5. Thickness Distribution of cancellous bone.

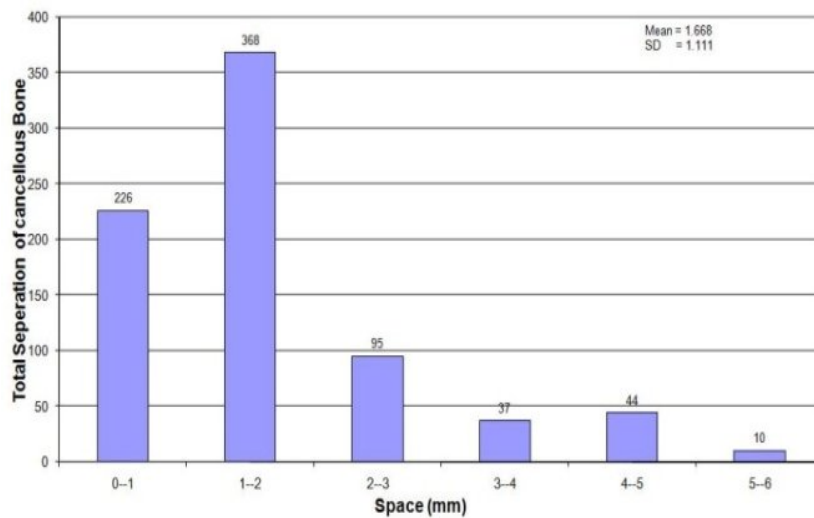


Figure 6. Separation distribution of cancellous bone.

The simulation result taken at region of interest (ROI) cancellous model only. From the simulation, figures 7, 8 and 9 show contour plots of pressure and velocity distribution of flow through cancellous bone with three models; actual, prismatic and QCS model, with mean value of gradient pressure across the specimen was found to be  $8.49298E-02\text{Pa}$  for actual model,  $9.07125E-02\text{pa}$  for prismatic model and  $6.19553E-02\text{ Pa}$  for quadratic crystal shape. The maximum velocity of actual model is  $7\text{ mm/s}$ , after the flow through the cancellous bone velocity will reduce become  $4.3\text{mm/s}$ . prismatic model have maximum velocity  $4\text{mm/s}$  and QCS model  $3.7\text{mm/s}$ , these result only representative for one model.

Velocity and pressure distribution were taken from every model shown figures 8 and 9 only at the centre model. This velocity will be used for calculating permeability of model. Normally velocity and pressure are calculated at the centre of model because at that position give higher accuracy for the analysis. The actual model gave higher velocity compared to other models. Generally, velocity and pressure profiles are the same for every model, when the model get the pressure drop the velocity will be reduced. Prismatic model shows more pressure drop compared the other models.

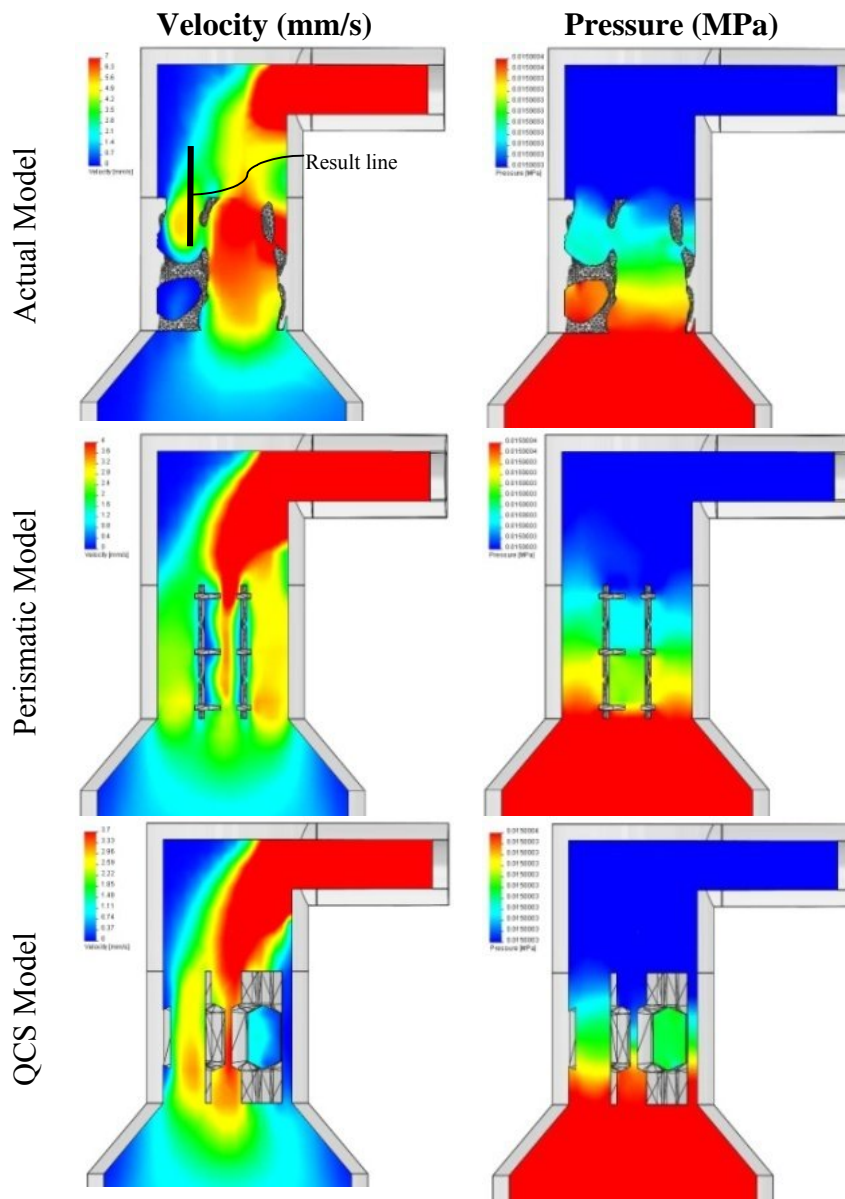


Figure 7. Contour plots of pressure and velocity distribution of flow through cancellous bone with three model; actual, prismatic and QCS model

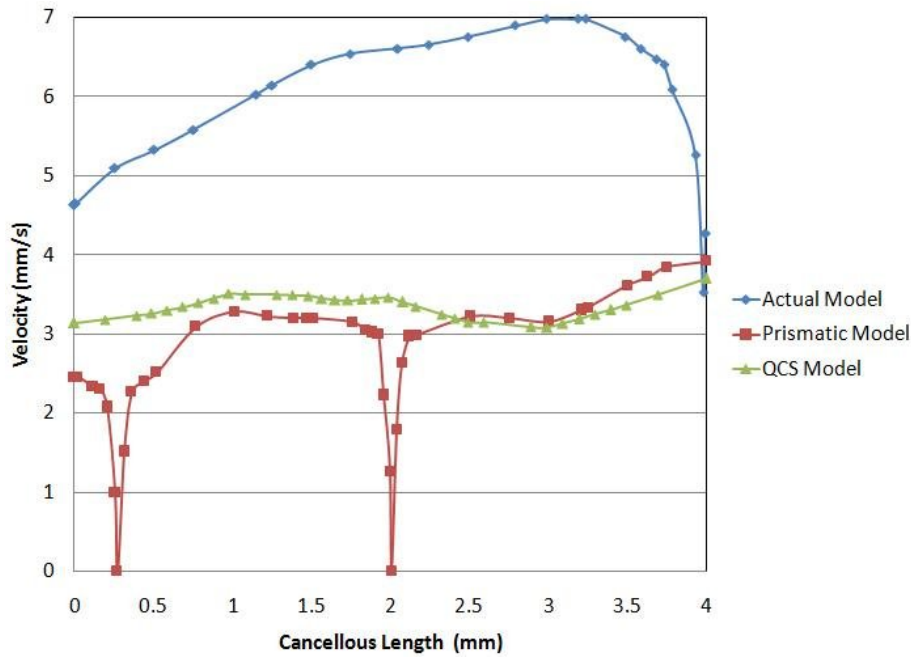


Figure 8. Velocity distribution of three model, the result taken from center of model (result line)

From the calculation of the specimen model of cancellous bone, it is shown that every model has different porosity. The range value of porosity 70% to 80% is actual model, 87% to 89.5% is prismatic model and 85% to 86% is quadratic crystal shape. The intertrabecular permeability for the all specimens ranged in order of magnitude from  $2.13E-05m^2$  to  $8.13E-08m^2$ . Permeability was calculated from at the centre only as in figure 10. Every type of model has difference between the minimum and maximum permeability. Actual model of permeability value in range  $1.99E-07m^2$  to  $1.01E-05m^2$ , prismatic model in range  $8.13165E-08m^2$  to  $1.35948E-05m^2$  and QCS model in range  $1.14E-05m^2$  to  $2.13E-05m^2$ , as depicted in figure 10.

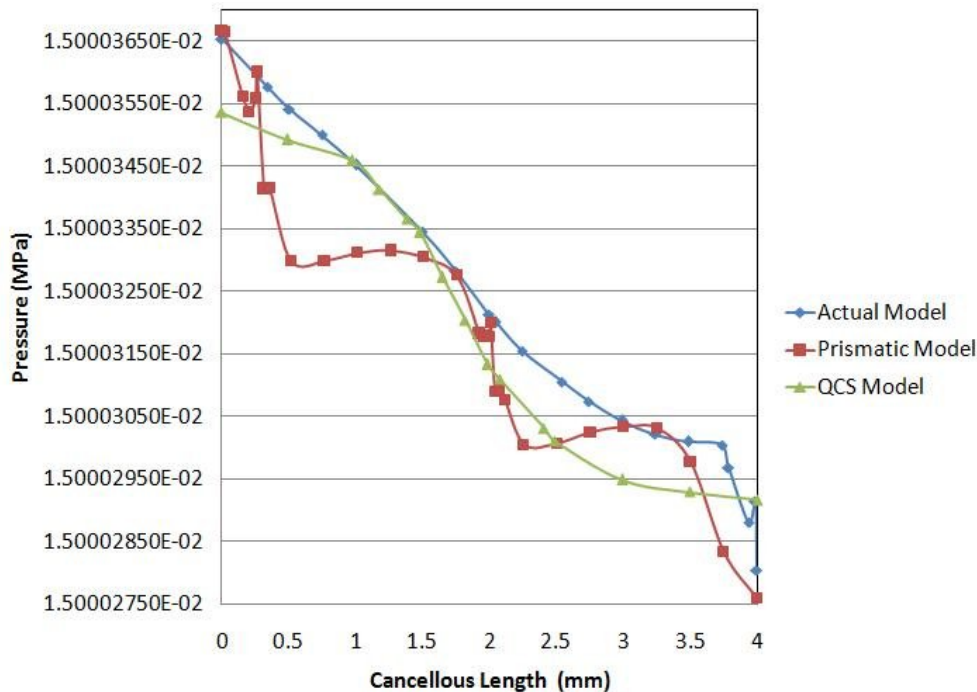


Figure 9. Pressure distribution of three model, the result taken from center of model (result line)

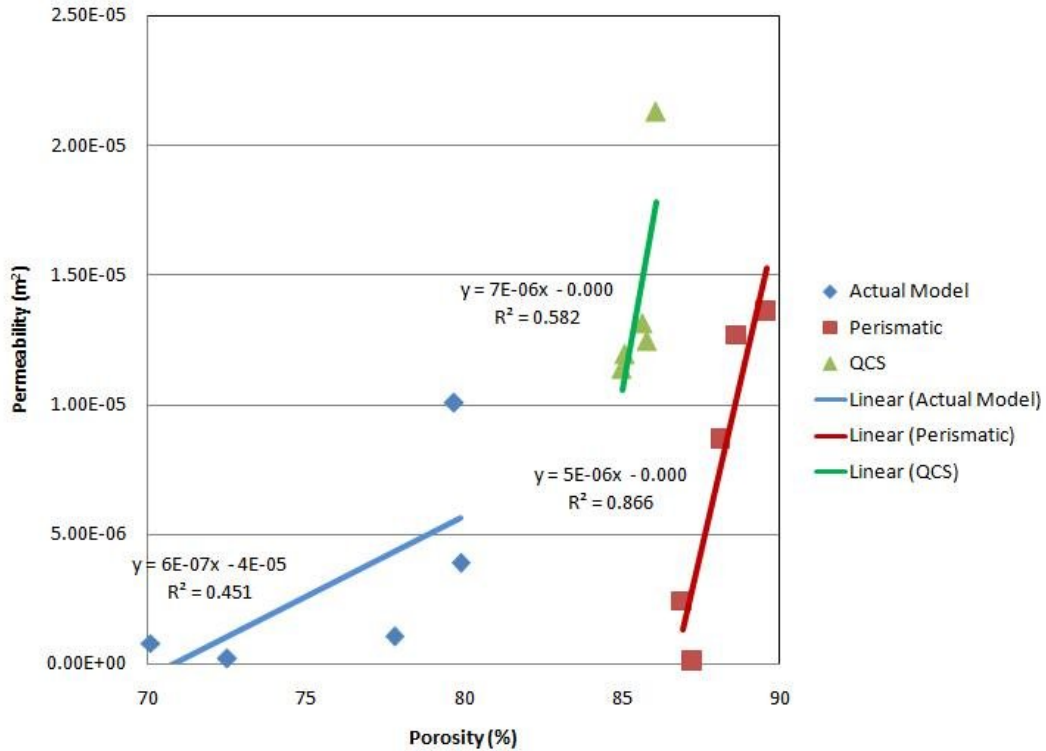


Figure 10. Cancellous bone permeability at three difference model

The dependence of permeability on porosity was complex and the porosity itself depended on anatomic side. Anatomic side depends on the location structure. Fig. 10 shown significant logarithmic regression at the  $R^2 = 0.866$  for prismatic model and last one is  $R^2 = 0.451$  for actual model. To that end, it is obvious that prismatic model have the highest dependence of porosity with permeability.

#### 4. Discussion

The simulation results show that the macroscopic permeability of the cancellous bone is not uniform. The central zone is more permeable than the periphery. This result was consistent with histological findings and qualitative studies from the literature.

The expression of the structure is a function of the relationship for the permeability of cancellous bone, which has the potential for application to design artificial trabecular bone. Permeability of cancellous bone is a factor affecting artificial cancellous bone as load bearing. From the simulation, we found permeability in the range of  $2.13 \times 10^{-5} \text{m}^2$  to  $8.13 \times 10^{-8} \text{m}^2$ , this value agrees well with previous researches. The differences in the result is because previous researchers used different fluid as medium, for this study the we have used blood as the fluid medium and another research using bone marrow [6, 11, 22] as fluid medium. From the present simulation we obtained more details about distributions of permeability at the specimen. Hence, the present simulation has capabilities to calculate the permeability easily at every point of the specimen.

Dependence of intertrabecular permeability on the structure [8], porosity, bone volume fraction, anatomic site [6, 7, 9-11, 22] and location taken of trabecular of each anatomic [13] have similarities with this simulation. Bone permeability (Fig. 10) increased in an over-proportional fashion with respect to porosity. This type of relation is not surprising because permeability is typically dependent on geometry in a higher polynomial fashion. These researches were more focused at the permeability as function to develop structures for replacing actual cancellous bone.

QCS model has higher permeability compared to the other model, but the porosity of prismatic structure is higher. It causes the structure of QCS to be more complex. That is immense relationship affects permeability with flow direction through of cancellous bone. Its complex structure will block the flow passing through the trabecular.

Characteristics of the flow through cancellous bone has implicated to the mimicked or artificial intertrabecular bone. Also, this permeability may have implication for the design of cemented prostheses total joint replacement and for clinical success of trabecular defect an optimal bone replacement must have a greater permeability than the surrounding bone [11]. The greater permeability as function transport properties for mass transfer or good nutrient supply. Normally when the permeability increases, the porosity becomes high, with this condition the trabecular bone is easier to get fractured. The ideal condition is a cancellous bone that has lower porosity but higher permeability. It's possible when the fluid flow pass through vertical direction. An example cemented prostheses replacement, best method to fill cement between cancellous bone with implant is vertical direction or longitudinal with the structure.

## 5. Conclusion

This study analysed the dependence of porosity on permeability of cancellous bone. Three models were reconstructed and developed (actual, prismatic and quadratic crystal shapes). Velocity and pressure distribution for the blood flow past the cancellous bone were plotted. Such distributions were provided as input data for calculating permeability for each model of cancellous bone. The results showed prismatic model to have similar permeability with actual model of cancellous bone. Quadratic and crystal shapes had the highest permeability of cancellous bone.

## References

1. Guggenbuhl, P., D. Chappard, M. Garreau, J.-Y. Bansard, G. Chales, and Y. Rolland, *Reproducibility of CT-based bone texture parameters of cancellous calf bone samples: Influence of slice thickness*. European Journal of Radiology, 2008. **In Press, Corrected Proof**.
2. Morita, M., A. Ebihara, M. Itoman, and T. Sasada, *Progression of osteoporosis in cancellous bone depending on trabecular structure*. Annals of Biomedical Engineering, 1994. **22**(5): p. 532-539.
3. Perie, D., D. Korda, and J.C. Iatridis, *Confined compression experiments on bovine nucleus pulposus and annulus fibrosus: sensitivity of the experiment in the determination of compressive modulus and hydraulic permeability*. Journal of Biomechanics, 2005. **38**(11): p. 2164-2171.
4. Kim, H.A., P.J. Clement, and J.L. Cunningham, *Investigation of cancellous bone architecture using structural optimisation*. Journal of Biomechanics, 2008. **41**(3): p. 629-635.
5. Teo, J.C.M., K.M. Si-Hoe, J.E.L. Keh, and S.H. Teoh, *Correlation of cancellous bone microarchitectural parameters from microCT to CT number and bone mechanical properties*. Materials Science and Engineering: C, 2007. **27**(2): p. 333-339.
6. Samuel, S.P., *Fluid/solid interactions in cancellous bone*. 2004, Cleveland State University: United States -- Ohio. <http://proquest.umi.com/pqdweb?did=885634721&Fmt=7&clientId=21690&RQT=309&VName=PQD>
7. Baroud, G., R. Falk, M. Crookshank, S. Sponagel, and T. Steffen, *Experimental and theoretical investigation of directional permeability of human vertebral cancellous bone for cement infiltration*. Journal of Biomechanics, 2004. **37**(2): p. 189-196.

8. Accadbled, F., D. Ambard, J.S. de Gauzy, and P. Swider, *A measurement technique to evaluate the macroscopic permeability of the vertebral end-plate*. Medical Engineering & Physics, 2008. **30**(1): p. 116-122.
9. Baroud, G., J.Z. Wu, M. Bohner, S. Sponagel, and T. Steffen, *How to determine the permeability for cement infiltration of osteoporotic cancellous bone*. Medical Engineering & Physics, 2003. **25**(4): p. 283-288.
10. Kohles, S.S., J.B. Roberts, M.L. Upton, C.G. Wilson, L.J. Bonassar, and A.L. Schlichting, *Direct perfusion measurements of cancellous bone anisotropic permeability*. Journal of Biomechanics, 2001. **34**(9): p. 1197-1202.
11. Nauman, E.A., K.E. Fong, and T.M. Keaveny, *Dependence of Intertrabecular Permeability on Flow Direction and Anatomic Site*. Annals of Biomedical Engineering, 1999. **27**(4): p. 517-524.
12. Mohammed Rafiq Abdul Kadir, Ardiyansyah Syahrom, and M.A.R. Yusof, *Microstructural Damage of Cancellous Bone Under Uniaxial Compression*. International Conference on ergonomics 2007, Kuala Lumpur, 2007(Biomechanics and Physiology): p. 32.
13. Mohammed Rafiq Abdul Kadir, Ardiyansyah Syahrom, and M.A.R. Yusof, *Micro-modelling and Analysis of Actual and Idealised Cancellous Structure*. 4 th Kuala Lumpur International conference on Biomedical engineering, 2008(Biomechanics ): p. 32.
14. Odgaard, A., *Three-dimensional methods for quantification of cancellous bone architecture*. Bone, 1997. **20**(4): p. 315-328.
15. Stauber, M. and R. Muller, *Volumetric spatial decomposition of trabecular bone into rods and plates--A new method for local bone morphometry*. Bone, 2006. **38**(4): p. 475-484.
16. Muller, R., H. Van Campenhout, B. Van Damme, G. Van der Perre, J. Dequeker, T. Hildebrand, and P. Ruegsegger, *Morphometric Analysis of Human Bone Biopsies: A Quantitative Structural Comparison of Histological Sections and Micro-Computed Tomography*. Bone, 1998. **23**(1): p. 59-66.
17. Kothari, M., T.M. Keaveny, J.C. Lin, D.C. Newitt, and S. Majumdar, *Measurement of intraspecimen variations in vertebral cancellous bone architecture*. Bone, 1999. **25**(2): p. 245-250.
18. Kim, H.S. and S.T.S. Al-Hassani, *A morphological model of vertebral trabecular bone*. Journal of Biomechanics, 2002. **35**(8): p. 1101-1114.
19. Xu, W., H. Zhang, Z. Yang, and J. Zhang, *Numerical investigation on the flow characteristics and permeability of three-dimensional reticulated foam materials*. Chemical Engineering Journal, 2008. **In Press, Corrected Proof**.
20. Singh, R., P.D. Lee, T.C. Lindley, R.J. Dashwood, E. Ferrie, and T. Imwinkelried, *Characterization of the structure and permeability of titanium foams for spinal fusion devices*. Acta Biomaterialia, 2008. **In Press, Corrected Proof**.
21. Despois, J.-F. and A. Mortensen, *Permeability of open-pore microcellular materials*. Acta Materialia, 2005. **53**(5): p. 1381-1388.
22. Grimm, M.J. and J.L. Williams, *Measurements of permeability in human calcaneal trabecular bone*. Journal of Biomechanics, 1997. **30**(7): p. 743-745.